Delft University of Technology

Robust Control

Assignment 1

Gerben Rijpkema 4686128
Jasper Boogers 4591704

December 13, 2021

Introduction

In this report, controllers are designed for a floating wind turbine (FWT). The FWT considered is modelled and linearized for a wind speed of 16 m/s to the linear time invariant model [4] given in Equation 1:

$$
\begin{aligned}
\dot{x} &= Ax + Bu \\
y &= Cx + Du \\
u &= [\beta, \tau_e, V]^T \\
x &= [\omega_r, \dot{z}_1, z_1, \dot{z}_2, z_2] \\
y &= [\omega_r, z]^T
\end{aligned}
$$

$$
\begin{aligned}
A &= \begin{bmatrix} -0.422 & -0.220 & 0.000 & -0.220 & 0.000 \\ 0.023 & -0.011 & -0.040 & -0.010 & 0.000 \\ 0.000 & 1.000 & 0.000 & 0.000 & 0.000 \\ 0.145 & -0.060 & 0.000 & -0.165 & -10.823 \\ 0.000 & 0.000 & 0.000 & 1.000 & 0.000 \end{bmatrix} \\
B &= \begin{bmatrix} -0.080 & -0.010 & 0.220 \\ -0.007 & 0.000 & 0.010 \\ 0.000 & 0.000 & 0.000 \\ -0.042 & 0.000 & 0.060 \\ 0.000 & 0.000 & 0.000 \end{bmatrix} \\
C &= \begin{bmatrix} 1 & 0 & 0 & 0 & 0 \\ 0 & 0 & 1 & 0 & 0 \end{bmatrix} \\
D &= 0
\end{aligned}
\tag{1}
$$

In this model, β represents the pitch angle of the blades in radians, τ_e the torque of the generator in MNm, ω_r the generator speed in rad/s and z the fore-aft tower top displacement of the wind turbine in meter. The third input of the model V represents the wind speed in m/s. Disturbances will act on this input channel, so this input cannot be used for control. The linearized state space model presented above will be used throughout the report.

To gain an understanding of the behaviour of the FWT, a first analysis will be made in Chapter 1 with regard to a single input, single output (SISO) system. Then, the analysis will be extended to multiple inputs and multiple outputs (MIMO). In Chapter 2, a multi-variate centralized controller is designed on the basis on Mixed-Sensitivity. In Chapter 3, a second multivariate controller is designed by further analysing the influence of the performance weights of a H_∞ controller.

1 SISO Analysis

In this first chapter, a first orientation is taken by investigating the model with respect to a single input and a single output (SISO) system. First, the plant is analysed in subsection 1.1, after which a controller is designed based on the requirements presented in subsection 1.2. The controller itself is designed in subsection 1.3. Lastly, time and frequency simulations are presented in subsection 1.4 to asses the performance of the controller.

The SISO analysis regards the relation of the first output ω_r to the first input β. The transfer function can be derived from the state space model given in Equation 1 and is given by Equation 2 below. This transfer function will be used troughout this chapter.

$$\frac{Y(s)}{U(s)} = \frac{-0.07988s^4 - 0.003315s^3 - 0.8677s^2 + 0.006493s - 0.03458}{s^5 + 0.5979s^4 + 10.98s^3 + 4.709s^2 + 0.5421s + 0.1827} \tag{2}$$

1.1 Investigation of SISO system behaviour

Figure 1 presents the open loop characteristics of the SISO system considered. In the left plot, the gain and phase shift of the plant are plotted. In the right plot, the poles and zeros are visualized. It can be noted that the Gain Margin is 24.2 dB at 0.2 rad/s and the Phase Margin is infinite. From Figure 1b a double Right Half Plane zero can be observed at $0.00385 \pm 0.2i$, as well as a double Left Half Plane pole at the same frequency. Both lead to a 180 degree phase loss individually, explaining the 360 degree phase loss in Figure 1a. This poses a limitation on the bandwidth of the controller, as sufficient distance from this phase loss is required. Therefore, the controller can only operate in the frequency range below 0.2 Hz. Lastly, various peaks in the open loop transfer function are noted, an indication of a high order system. This can be verified by inspecting the transfer function above in Equation 2.

As the open loop magnitude never reaches -3dB, a high bandwidth is never achieved. For a PID controller, this indicates the need for s proportional or integral gain. The two inverted peaks of the gain at 0.2 rad/s and 3.29 rad/s may also become problematic when trying to achieve a high bandwidth. An idea would be to try pole-zero cancellation, but this may cause internal instability. In either case, as the phase loss of the system is 360 degrees beyond 0.2 rad/s, control beyond that frequency is not regarded as feasible. This severe phase loss is due to the double RHP zero visualized in Figure 1b.

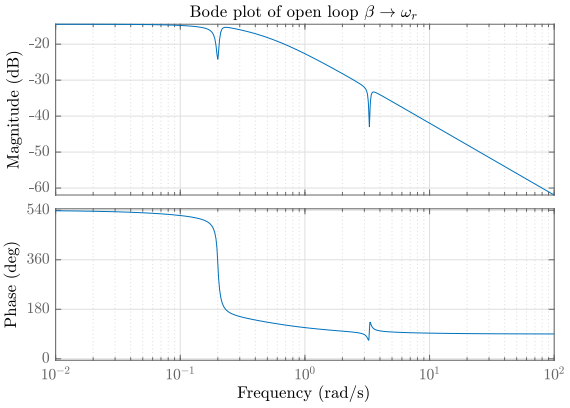

(a) Bode Plot of the plant.

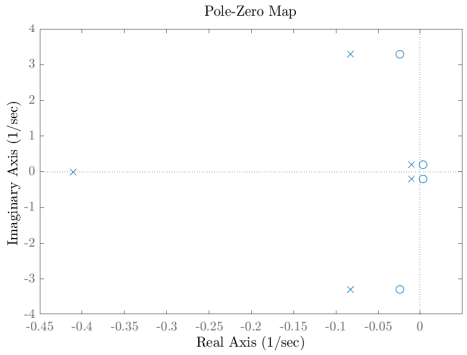

(b) Pole-Zero Plot of the plant.

Figure 1: Open loop characteristics of the SISO system.

1.2 Defining controller requirements

To gain an understanding of the behaviour of the FWT, a controller is set up. In the time domain, the following requirements were set up for the controller:

1. Small settling-time.

2. Overshoot $< 1\%$.

3. No steady state error.

To implement these requirements in a SISO controller, a loop shaping approach is taken. Started is by translating the time-domain design requirements into frequency-domain design requirements on the transfer functions:

1. Small settling time relates to a large bandwidth, so the frequency where the closed-loop gain first crosses $1/\sqrt{2}$, should be large. It is however limited by the RHP zeros.

2. The overshoot is related to the resonant peak M_r of the complementary sensitivity function, which should thus be small.

3. No steady state error relates to a gain of 1 of the complementary sensitivity function for frequencies $\to 0$.

The next step is to find the desired gain cross-over frequency for tracking of the reference. This is defined as the frequency where the gain of the loop transfer function crosses 0 dB from below [2]. The desired cross-over frequency is dependent on the desired behaviour of the FWT. Typically, wind turbines operate in the range of < 1 Hz. In subsection 1.1 it was also shown that there was a limitation on controlling the FWT due to a phase loss of 360 degrees beyond 0.2 rad/s. For these reasons, the cross-over frequency is chosen to be in the range of 10^-1 rad/s.

1.3 Controller design and assessment

Now that the goals for the transfer functions are clear, the controller can be designed. The layout of the chosen controller is presented in Figure 2.

From the third requirement in subsection 1.2, it can be noted that this controller should have a nonzero I component. This will cause the complementary sensitivity to have a gain of approximately 1 for frequencies $\to 0$.

The gains of the controller are tuned by inspecting the resulting loop transfer functions for different controller parameters. During this iterative loop shaping process, it is observed that placing a double complex zero around 0.2 rad/s results in large gain margin, as well as providing a high phase margin. This relates to the implementation of the Integrator component for reference tracking. For noise attenuation, a pole is placed at -1. This corresponds to the Derivative component of the controller. The Proportional gain of the controller was chosen to be zero. This results in a PID controller with $K_p = 0$, $K_i = -0.39$, $K_d = -9.75$, $T_f = 1$.

Figures 3 and 4 present the corresponding closed loop Bode plot and step response, as well as the (complementary) sensitivity of the system. The time and frequency response characteristics are presented in Table 1. The presence of RHP zeros is indicated in the step response plot by the partial amplitude drop after the initial rise, which suggests a non minimum phase system. The authors recognise that the presented controller is somewhat non-conventional. An alternative controller could for example be derived with a Ziechler-Nichols approach. Nonetheless, the presented performance parameters do suggest that the controller functions well.

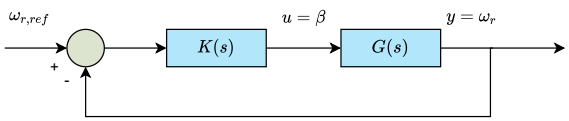

Figure 2: Block diagram of the SISO system.

Characteristic	Value
Rise Time	27.58 s
Settling Time	36.05 s
Overshoot	0.90%
Steady State Error	0
Bandwidth	0.091 Hz
Gain Margin	32.3 dB (at 0.032 Hz)
Phase Margin	78.5 deg (at 0.010 Hz)

Table 1: Performance of SISO controller.

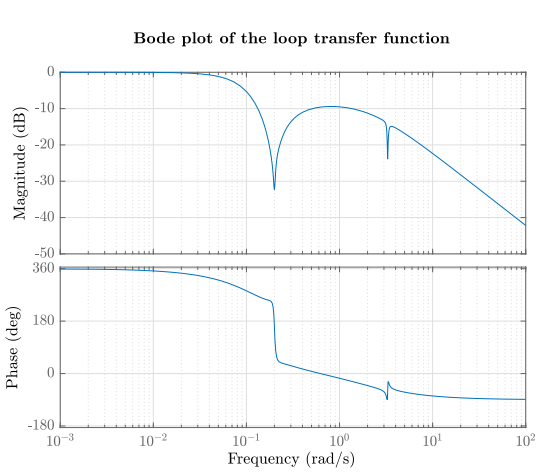

(a) Bode Plot of the loop transfer function.

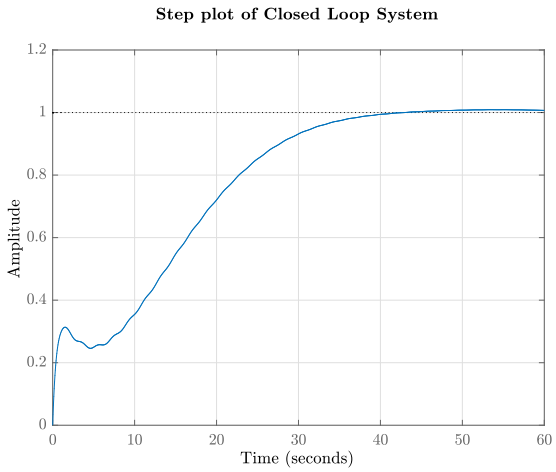

(b) Step response of the closed loop system.

Figure 3: Closed loop characteristics of the SISO system.

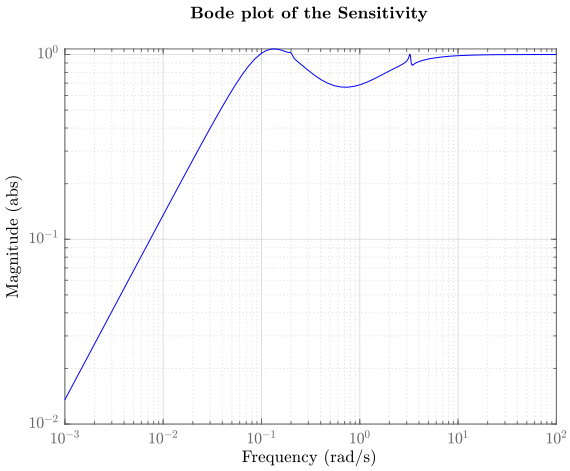

(a) Sensitivity of the closed loop system.

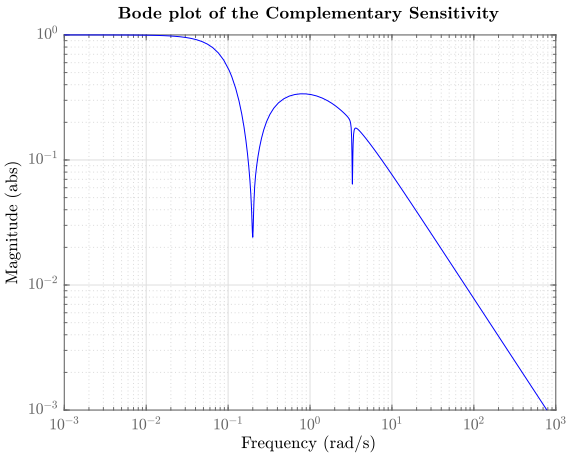

(b) Complementary Sensitivity of the closed loop system

.

Figure 4: Closed loop sensitivity assessment of the system.

1.4 Disturbance rejection

To inspect the performance of the derived controller of the previous subsection, a time domain simulation is executed. Figure 5 presents the response of the system when the third channel of the MIMO system (V) is excited using a unit step signal. This simulates a disturbance of the wind speed around the linearization point [4]. The significant overshoot and large settling time indicate that this controller is not suitable for disturbance rejection. A larger Derivative action may result in a better performance. Another possibility to improve performance is to also use τ_e to control the plant. This approach is taken in the next chapters.

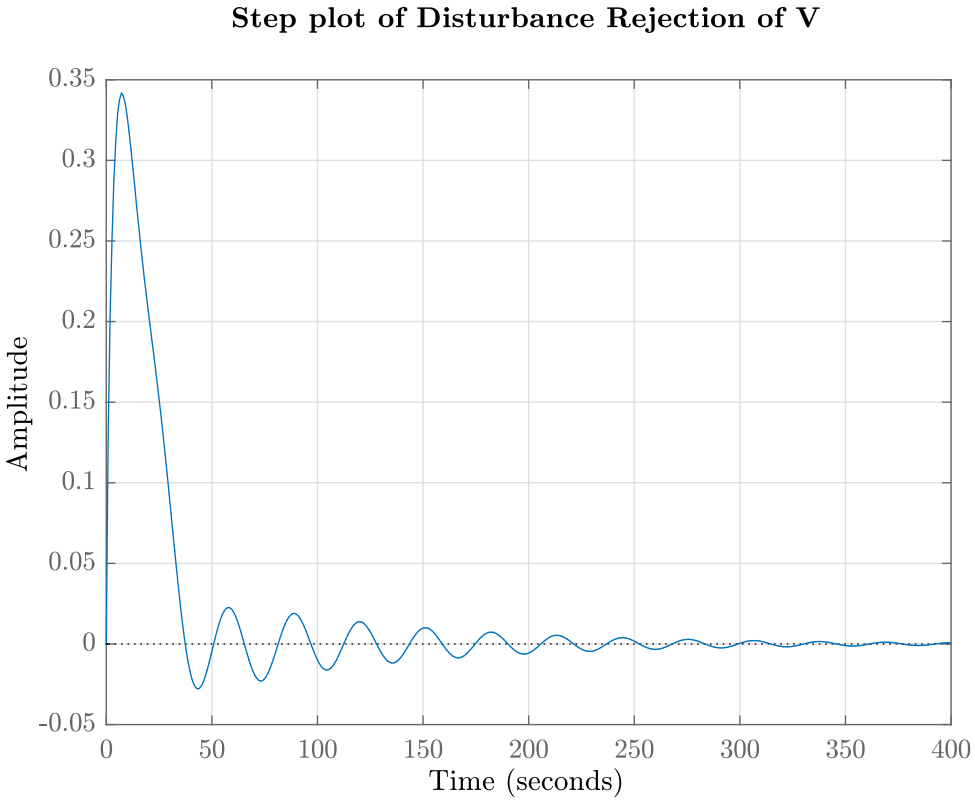

Figure 5: Disturbance rejection response of SISO controller.

2 MIMO Sensitivity Analysis

In this chapter, the analysis of the FWT system is extended to both the inputs β, τ_e and both the outputs ω_r and z. A centralized MIMO controller is designed based on mixed-sensitivity. The mathematical formulation of the design problem is defined as:

$$\min_K \|N(K)\|_\infty; \qquad N = \begin{bmatrix} W_P S \\ W_u K S \end{bmatrix} \tag{3}$$

Here, W_u, W_p respectively denote the chosen performance weights on the plant input and output. S denotes the sensitivity function. The H_∞ optimal controller K is given as the minimizing argument of the optimization problem.

To start, an analysis is made of the open loop transfer function by first analysing the relative gain array of the plant and secondly analysing the MIMO poles and zeros. Thirdly, the desired filters for the performance outputs are determined. After this, a block diagram of the system including the controller is given. Subsequently, the system is reformulated into a generalized plant problem. Next, the performance weights are analyzed qualitatively. Afterwards, the controller is set up by optimizing the H_∞ norm of the mixed sensitivity. Finally, the performance of the controller is simulated in the time domain.

2.1 Gain analysis of MIMO open loop

Firstly, the relative gain array (RGA) of the plant is inspected, which can be computed using

$$\text{RGA}(G(s)) = G(s) \times \left(G^{-1}(s)\right)^T \tag{4}$$

Here, $\times$ denotes the Hadamard product [3]. Computing the RGA can yield insight in the two-way interaction of the system and indicates sensitivity to uncertainty [1]. For the FWT, the RGA is inspected for 0 Hz and 0.4 Hz to analyze both the steady state and crossover-frequency region. For the frequency $\omega = 0$ Hz, the RGA is given by:

$$\begin{bmatrix} -0.092 & 1.092 \\ 1.092 & -0.092 \end{bmatrix} = \begin{bmatrix} -0.707 & 0.707 \\ 0.707 & 0.707 \end{bmatrix} \begin{bmatrix} 1.184 & 0.000 \\ 0.000 & 1.000 \end{bmatrix} \begin{bmatrix} 0.707 & 0.707 \\ -0.707 & 0.707 \end{bmatrix}^T \tag{5}$$

In the right hand side, the singular value decomposition of the RGA is given. For $\omega = 0$, the maximum and minimum singular value are given by $\bar{\sigma} = 20.811$, $\underline{\sigma} = 0.111$ respectively. The range between the maximum singular value and the minimum singular value is relatively high. The condition number equals $\gamma = \bar{\sigma}/\underline{\sigma} = 187$, which can indicate control issues. For the frequency $\omega = 0.4$ Hz $= 0.8\pi$ rad/s, the RGA is given by:

$$\begin{bmatrix} -0.655 & 1.655 \\ 1.655 & -0.655 \end{bmatrix} = \begin{bmatrix} -0.707 & 0.707 \\ 0.707 & 0.707 \end{bmatrix} \begin{bmatrix} 2.311 & 0.000 \\ 0.000 & 1.000 \end{bmatrix} \begin{bmatrix} 0.707 & 0.707 \\ -0.707 & 0.707 \end{bmatrix}^T \tag{6}$$

For $\omega = 0.4 * 2\pi, \bar{\sigma} = 1.282, \underline{\sigma} = 0.923$. Now, the range between the minimum and maximum singular value is smaller. The condition numer is $\gamma = 1.39$. This means that the multivariable effects of uncertainty are most likely not a problem for this frequency. For both the RGA $\omega = 0, \omega = 0.8\pi$, it is noted that the off diagonal terms are relatively close to 1 and the diagonal terms are negative. Therefore, pairing the inputs (u_1, y_2) and (u_2, y_1) [3] may result in a well-functioning decentralized controller [1]. This corresponds to pairing blade pitching to fore-aft tower motion and using the generator torque to control the generator speed.

2.2 Pole and zeros analysis

To inspect limitations on the MIMO performance, the zeros and poles of the transfer function of the plant are inspected. Using MATLAB, the following MIMO zeros and poles are found. For the zeros, the rank of the

transfer function of the plant is less than the original rank of the transfer function of the plant.

$$\begin{bmatrix} p_1 \\ p_2 \\ p_3 \\ p_4 \\ p_5 \\ p_6 \end{bmatrix} = \begin{bmatrix} -0.083 + 3.294i \\ -0.083 - 3.294i \\ -0.410 + 0.000i \\ -0.011 + 0.202i \\ -0.011 - 0.202i \end{bmatrix} \qquad \begin{bmatrix} z_1 \\ z_2 \end{bmatrix} = \begin{bmatrix} -0.008 + 1.236i \\ -0.008 - 1.236i \end{bmatrix} \tag{7}$$

The presence of zeros are at 0.2 Hz and indicate that there is a combination of inputs that may render the system unobservable. This will result in control limitations above this frequency, as for an unobservable system it is not possible to guarantee internal stability, which is undesirable.

2.3 Selecting of performance weights

Now that the first steps have been made in analyzing the MIMO plant, the performance weights for the H_∞ synthesis can be designed. The plant again has output y and input u. The generalized disturbance is defined as the vector w of length 2. The performance signals z and performance weights W are now defined as given below.

$$y = \begin{bmatrix} \omega_r \\ z \end{bmatrix}$$
$$u = \begin{bmatrix} \beta \\ \tau_e \end{bmatrix}$$
$$z = \begin{bmatrix} z_1 \\ z_2 \end{bmatrix} = \begin{bmatrix} W_p(y+w) \\ W_u u \end{bmatrix}$$

$$W_p = \begin{bmatrix} W_{p11} & 0 \\ 0 & 0.2 \end{bmatrix} \tag{8}$$

$$W_u = \begin{bmatrix} 0.01 & 0 \\ 0 & \frac{5\cdot10^{-3}s^2+7\cdot10^{-4}s+5\cdot10^{-5}}{s^2+14\cdot10^{-4}s+10^{-6}} \end{bmatrix} \tag{9}$$

It can be seen that a decentralized approach was taken as the off-diagonal terms are zero. W_{p11} relates to the desired weight for the first output channel ω_r. The goal is set to design a weight on this to have a cut-off frequency of $\omega_B = 0.4$ Hz $= 0.8\pi$ rad/s, an attenuation of low-frequency disturbances of $A_i = 10^{-4}$ and an H_∞ norm of the sensitivity function of $M_i = 1.8$. These requirements can be translated into the following transfer function [3],

$$w_{p,i} = \frac{\frac{s}{M_i} + \omega_{Bi}}{s + \omega_{Bi}A_i} \tag{10}$$

$$W_{p11} = \frac{0.556s + 0.8\pi}{s + 0.8\pi \cdot 10^{-4}} \qquad \rightarrow \qquad W_p = \begin{bmatrix} \frac{0.556s+0.8\pi}{s+0.8\pi\cdot10^{-4}} & 0 \\ 0 & 0.2 \end{bmatrix} \tag{11}$$

2.4 Block diagram of plant

To create an overview of the signals and transfer function related to the H_∞-synthesis, a block diagram was created. This is presented in Figure 6

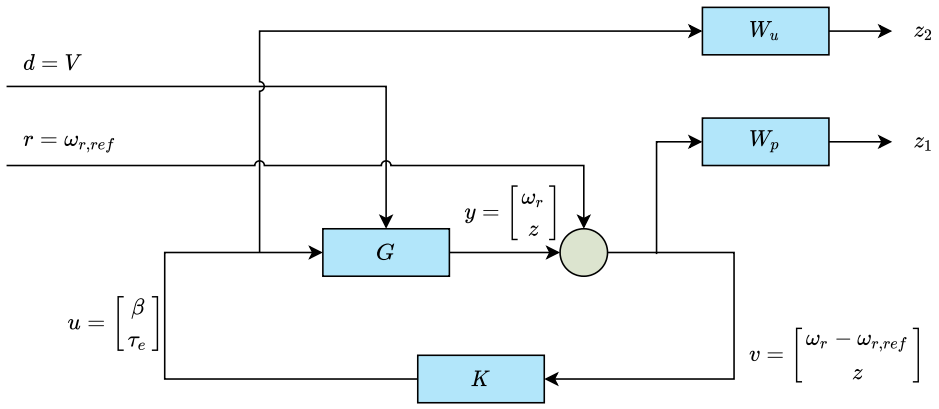

Figure 6: Block diagram of the plant under consideration.

2.5 Generalization of plant

The block diagram of the system above can also be generalized into a generalized plant. A block diagram of this is presented in Figure 7. Taking two control outputs z and two disturbance inputs w as well as 2×2 performance outputs z and two control inputs u leads to a generalized plant with 6 outputs and 4 inputs. Taking 5 states from the plant combined with one first order weight and one second order weight results in a generalized plant with 8 states. Both the in- and outputs as well as the number of states are verified using MATLAB.

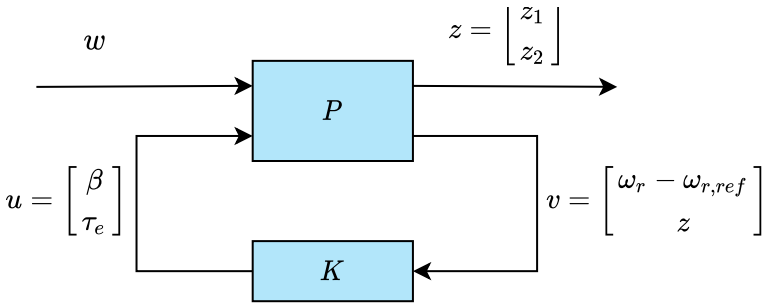

Figure 7: Block diagram of the Generalized Plant.

$$\begin{bmatrix} z \\ y \end{bmatrix} = \begin{bmatrix} P_{11} & P_{12} \\ P_{21} & P_{22} \end{bmatrix} \begin{bmatrix} w \\ u \end{bmatrix} \tag{12}$$

$$P_{11} = \begin{bmatrix} W_p \\ 0 \end{bmatrix} \tag{13}$$

$$P_{12} = \begin{bmatrix} W_p G \\ W_u \end{bmatrix} \tag{14}$$

$$P_{21} = I \tag{15}$$

$$P_{22} = G \tag{16}$$

$$P = \left[\begin{array}{c|c} P_{11} & P_{12} \\ \hline P_{21} & P_{22} \end{array}\right] = \left[\begin{array}{c|c} W_P & W_P G \\ 0 & W_u \\ \hline I & G \end{array}\right] \tag{17}$$

2.6 Relation of performance weights to physical system

As described in subsection 2.3, the following performance weights for chosen.

$$W_u = \begin{bmatrix} 0.01 & 0 \\ 0 & \frac{5\cdot10^{-3}s^2+7\cdot10^{-4}s+5\cdot10^{-5}}{s^2+14\cdot10^{-4}s+10^{-6}} \end{bmatrix} \tag{18}$$

$$W_p = \begin{bmatrix} \frac{0.556s+0.8\pi}{s+0.8\pi\cdot10^{-4}} & 0 \\ 0 & 0.2 \end{bmatrix} \tag{19}$$

$$\tag{20}$$

Considering W_p, The second output of the system z is multiplied with a constant gain of 0.2. The error in ω_r is multiplied with a transfer function of which the Bode plot is presented in Figure 8a. By design, this transfer function W_{p11} amplifies frequencies $\omega < 0.8\pi$ and attenuates other frequencies. This implies that the controller should not act on high frequency errors in ω_r but the steady state error should be zero.

In W_u, it can be seen that the first input, β is multiplied with a constant gain of 10^{-2}. The second input τ_e is multiplied with a transfer function of which the Bode plot is shown in Figure 8b. It can be seen that this function amplifies frequencies $\omega < 10^{-2}$ rad/s and attenuates frequencies $\omega > 10^{-2}$ rad/s. Thus, for low frequencies, the usage of τ_e for control is penalized. This corresponds to the requirement that steady state contribution of the generator torque for control should be absent.

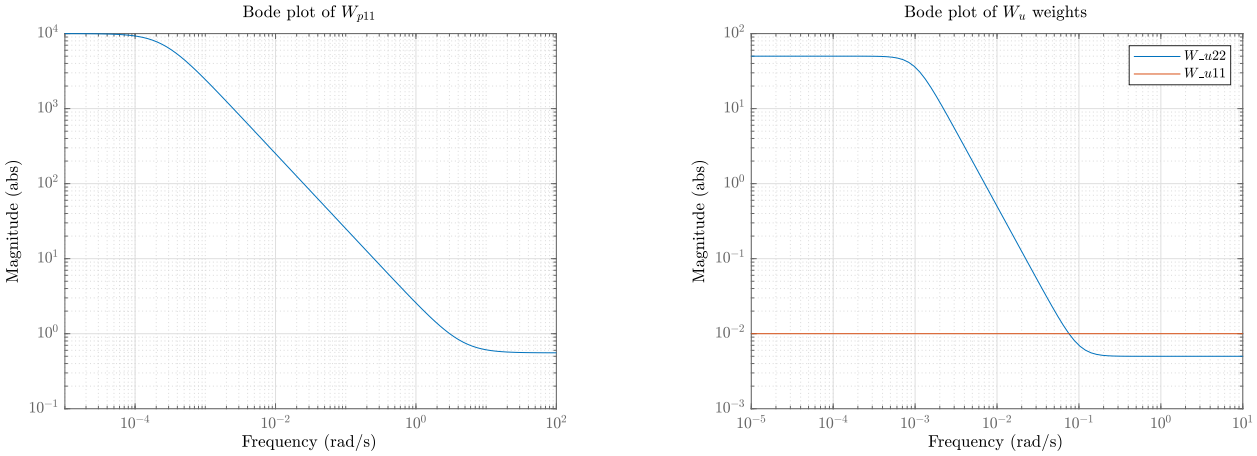

(a) Weights on output

(b) Weights on input

Figure 8: Weights on the performance channels

2.7 Mixed-sensitivity generalized controller design

Now that the design problem has been formulated, the optimization can be executed. This is done via the `hinfsyn` command of MATLAB. This results in a resulting norm of:

$$\min_K \|N\|_\infty = \gamma = 0.80 \tag{21}$$

As the norm is below 1, the synthesis was successful.

However, when looking at the poles of the resulting controller, two RHP poles can be found, so it can be concluded that the controller is unstable. The RHP poles cancel the RHP zeros of the plant, resulting in a stable loop transfer function.

To check the closed loop stability of the resulting controller, a generalized nyquist analysis is performed. The contour map of the determinant of $I + L(s)$ is given in Figure 9a. In Figure 9b two encirclements of the critical point can be observed. As the controller has two RHP poles, the resulting closed loop will be stable.

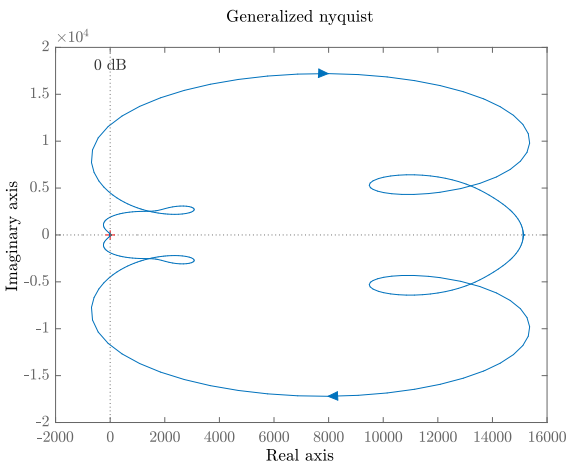

(a) Nyquist plot of the open loop system.

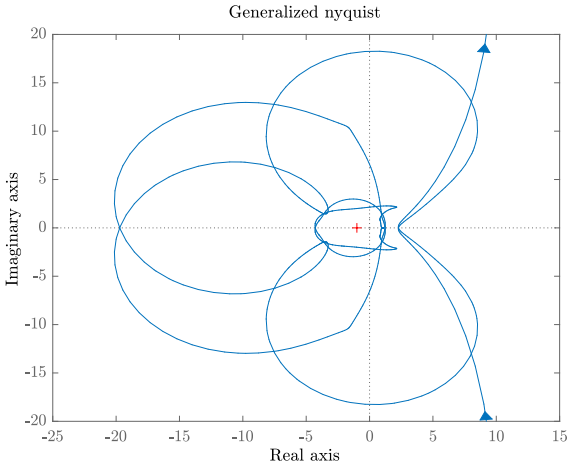

(b) Nyquist plot zoomed in on origin.

2.8 Time domain simulation of controller

A step response of the controlled system is presented in Figure 10 for both reference tracking of ω_r and disturbance rejection for the wind speed V. The disturbance response of τ_e will have a significant effect on the power production, based on the significant overshoot peak and long settling time.

Concluding, even though τ_e can be used in the scenario considered, it is very hard to make use of this variable without significantly altering the power produced. Also, two RHP poles render the controller unstable and as internal stability is not desired, the controller is not regarded practically implementable.

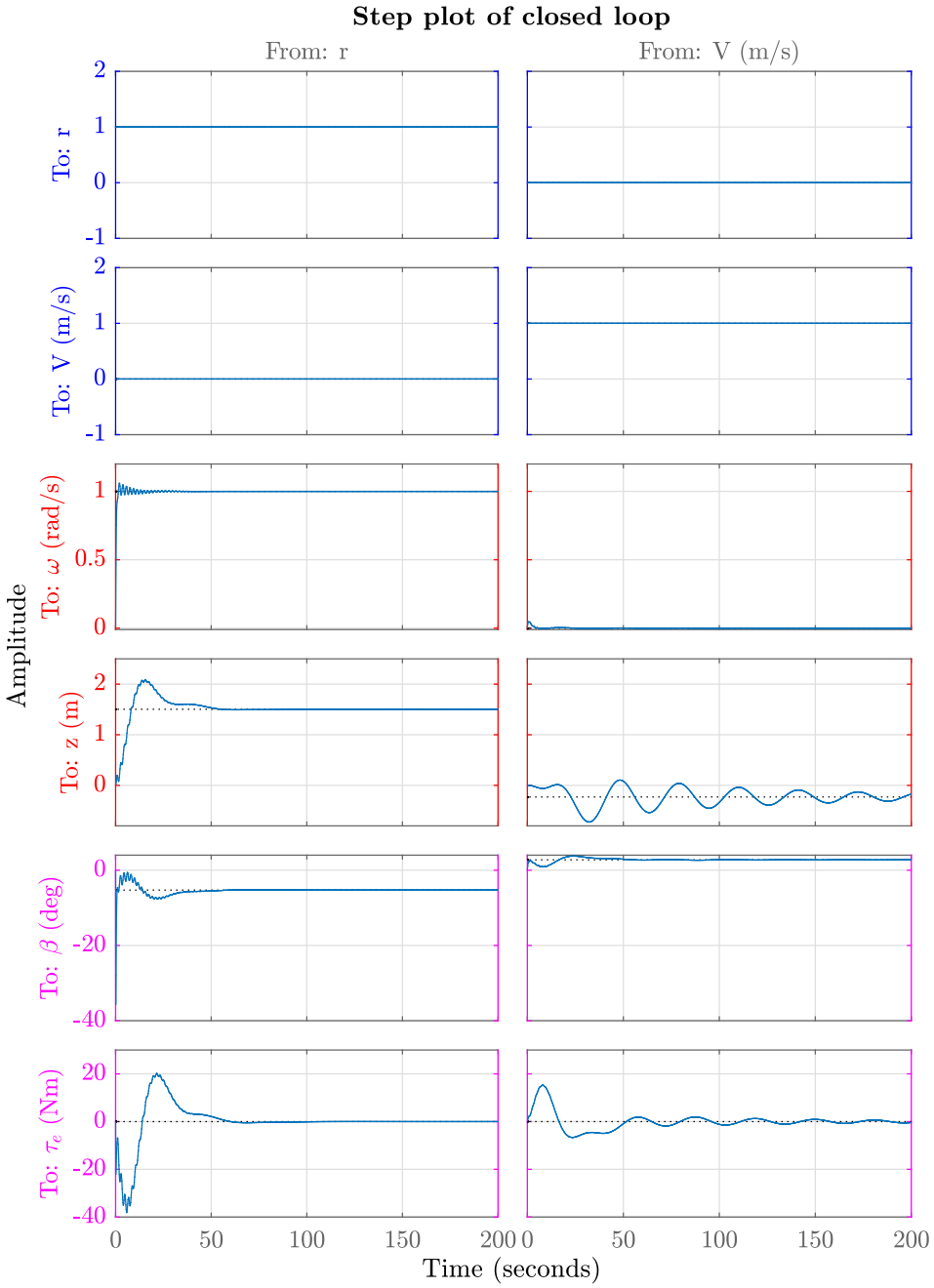

Figure 10: Reference tracking and disturbance rejection of the controlled MIMO system.

3 MIMO Weighting Design

In this chapter an alternative approach will be taken to again design a multivariate controller for the FWT.

The situation will be assessed where the the FWT is running at its rated power of $P_{rated} = 1.8$ MW. Therefore, $\tau_e \omega_r = 1.8$ MW continuously can be used as a performance goal. Again, the two inputs β, τ_e are available for control and V acts as a disturbance on the system. From the outputs, now only ω_r will be regarded. The controller itself will again be designed using H_∞-synthesis; minimizing $\| \begin{bmatrix} W_P S \\ W_u K S \end{bmatrix} \|_\infty$.

Firstly, the generalized plant for the new problem is set up. Secondly, the weights are selected for the output dynamics. Thirdly, new weights are selected for the control inputs. Afterwards, the controller is synthesized and the resulting loop transfer functions are inspected visually. Finally, a time simulation of the controller is executed based on actual wind data.

3.1 Generalized plant

The new generalized plant has exogenous input w (1x1) and exogenous output z. w functions as generalized disturbance. The input signal for control v equals the error value defined as $e = \omega_r - 0$. The control signals are $u = [\beta, \tau_e]^T$ (2x1).

The control values u are weighted with W_u, resulting in z_2 being of size 2x1. The error v is weighted with W_p, resulting in z_1 being a scalar. Therefore, $z = [z_1, z_2]^T$ is a vector of length 3. A block diagram of the generalized plant is given in Figure 11.

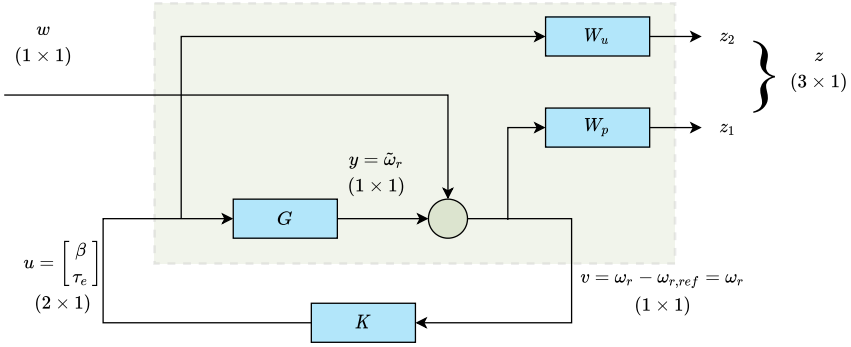

Figure 11: Generalized plant for MIMO weighting design.

3.2 Error weighting

To execute the H_∞ design problem, the performance weights have to be designed. In this subsection, the weight on the output error channel is designed. This weight is defined as W_P and determines in which region accurate control is desired. The output error was defined as the deviation of the rotational velocity ω_r from the linearization point of $\omega_r = 0$ rad/s.

In subsection 2.2, it was determined that there is a performance limitation of controlling the rotational velocities for frequencies above 0.2 Hz. In subsection 2.3, a transfer function for the performance output channel ω_r of the plant considered in section 2 was derived. This transfer function was built to attenuate low frequency disturbances in the rotational velocity of the FWT. The cut-off frequency was chosen as 0.4 Hz. Due to the performance limitation on high frequency control, this transfer function again would a good option. Therefore, W_P is defined once more as:

$$W_p = \frac{0.556s + 0.8\pi}{s + 0.8\pi \cdot 10^{-4}} \tag{22}$$

3.3 Controller weighting

The controller weights are defined as W_u in Figure 11. These weights are used to penalize the usage in regions where the physical usage of a specific input channel is not preferred. For the FWT, the generator

torque τ_e is best suited for high frequency regions, as blade pitching by controlling β is slow. On the other hand, using β is ideal for low frequency control as it does not directly affect the power production of the FWT [4]. Therefore, penalties can be implemented via a high weight on the first input for low frequencies and a high weight on the second input for high frequencies, resulting in a low and high pass filter respectively. Again, a decentralized controller is chosen. Thus, the off diagonal terms of W_u are equal to zero.

The exact weighting depends on the control cost of each control input for the relevant frequencies. In this report it is assumed that this cost can be implemented via a first order filters with cut-off frequencies ω_{c1}, ω_{c2}. The matrix W_u is therefore selected as:

$$W_u = \begin{bmatrix} \frac{\omega_{c,1}}{s+\omega_{c,1}} & 0 \\ 0 & \frac{s}{s+\omega_{c,2}} \end{bmatrix} \tag{23}$$

The values for ω_{c1}, ω_{c2} can depend on the exact equipment used for the FWT. In this report, the following values were chosen as $\omega_{c,1} = 0.3 \cdot 10^{-3}$ rad/s and $\omega_{c,2} = 1 \cdot 10^{-1}$ rad/s. Bode plots of each of the weights are presented in Figure 12.

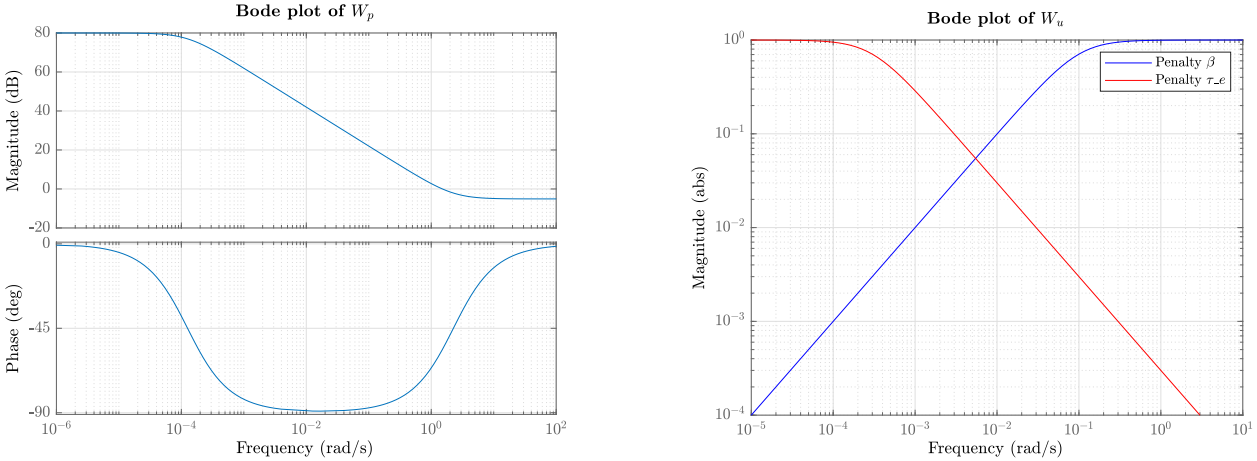

(a) Weights on error channel.

(b) Weights on control inputs.

Figure 12: Selected Weights for MIMO weighted design.

3.4 Controller synthesis

With MATLAB, the H_∞ synthesis is executed with the weights and generalized plant as stated in the sections above. This resulted in a norm of:

$$\min_K \|N\|_\infty = \gamma = 0.86 \tag{24}$$

As the norm is below 1, the synthesis was successful. This can also be seen from the plots below. The output lines of the system lie below the inverse of the weights for all the performance channels, which indeed indicates a successful optimization.

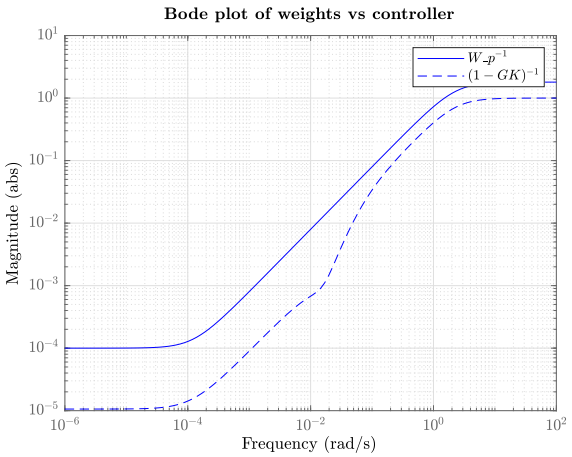

(a) Comparison for control input channels.

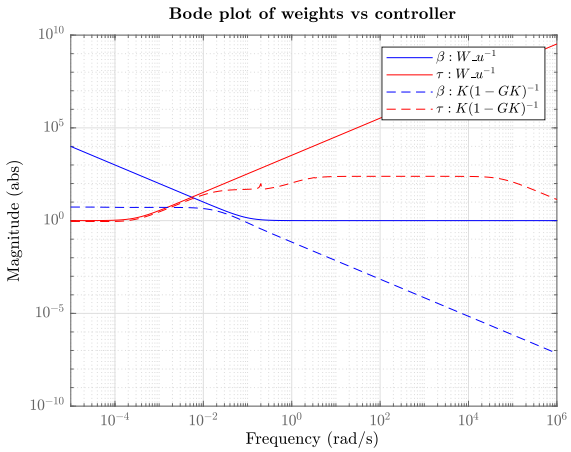

(b) Comparison for error channel.

Figure 13: Comparison of performance weights to derived controller.

3.5 Controller Simulation

To analyze the performance of the third controller that was derived in this section, again a time-domain simulation was executed. However, unlike simulating a step response, the response was calculated to a more complex wind speed input, visualized in Figure 14 below. From the data, visualized in blue, a high frequency and low frequency part can be seen. To gain an understanding of the behaviour of the controller, the system is simulated with two inputs. For Simulation 1, the wind speed input is taken as both the high and low frequency part. For Simulation 2, only the low frequency part of the input is taken, given by $V_2 = 2\sin(2 \cdot 10^{-3}\pi t)$.

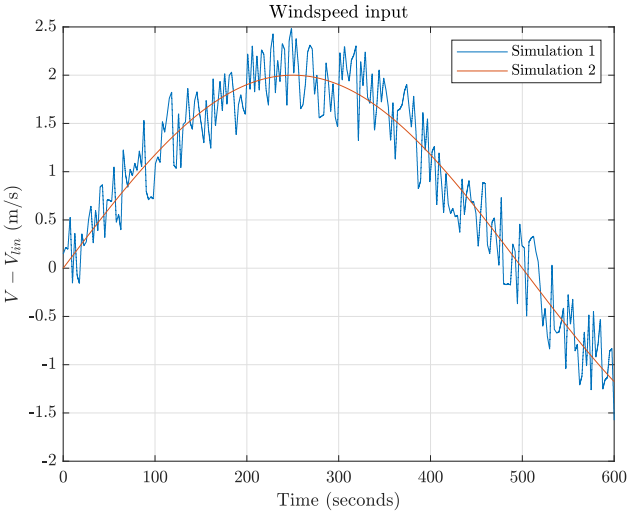

Figure 14: Input wind data of simulation.

The resulting dynamics of the FWT for the derived controller of this section are given Figure 15. It can be observed that the the blade pitch angle β only acts on low-frequent inputs, while the generator torque reacts on the high frequency disturbances.

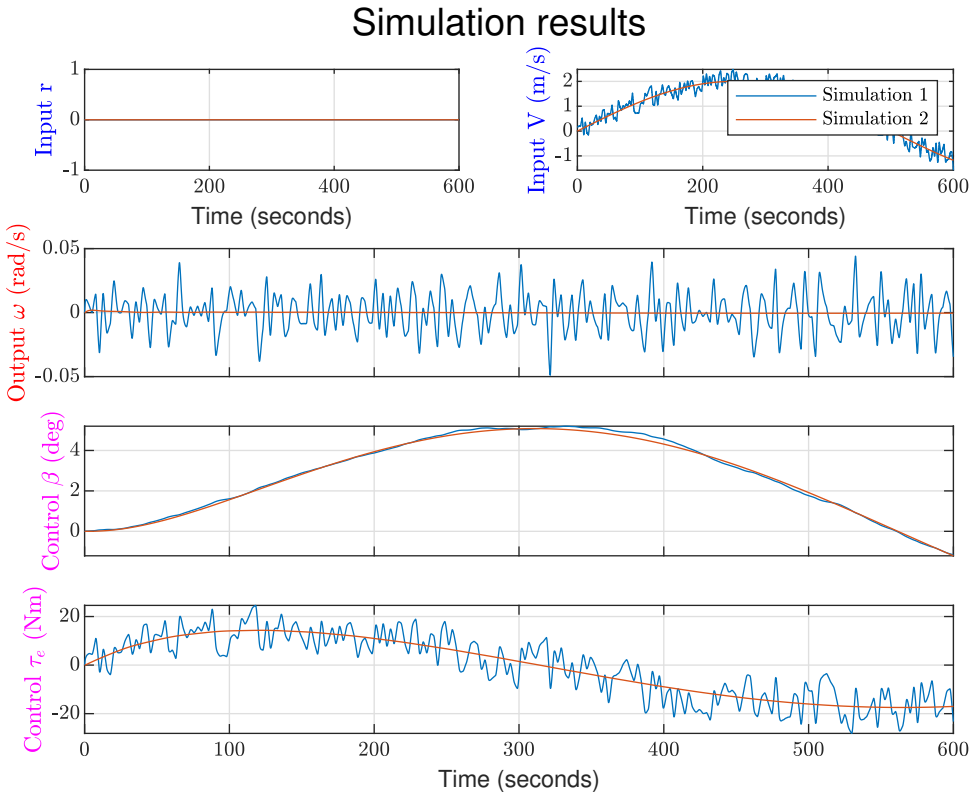

Figure 15: Simulation results of the provided wind data.

There is still a low frequent part in the control of τ_e with a magnitude of about 20 Nm. An attempt to eliminate this last low frequent part resulted in either H_∞ norms far larger than 1 or , thus rendering the controller unsuitable for the design requirements. However, to put the presented values in perspective: the rated generator torque is 10^4 Nm, thus a sinusoidal response with an amplitude of 20 Nm is regarded within reasonable limits for this control problem.

Concluding, the design goals of only using β for low frequency control and using τ_e for high frequency control seem to be achieved. The controller responds reasonable for disturbance rejection of a varying wind speed V.

References

[1] Sigurd Skogestad and Ian Postlethwaite. *Multivariable Feedback Control: Analysis and Design*. Wiley, 2010.

[2] Róbert Ungurán et al. "Feedback-feedforward individual pitch control design for wind turbines with uncertain measurements". In: *2019 American Control Conference (ACC)*. 2019, pp. 4151–4158. DOI: 10.23919/ACC.2019.8814757.

[3] J.W. van Wingerden. *Lecture Slides on Robust Control [SC42145]*. Technische Universiteit Delft. 2021.

[4] J.W. van Wingerden. *Practical Assingment: Control Design for a Floating Wind Turbine [SC42145]*. Technische Universiteit Delft. Oct. 2021.

Appendix

The MATLAB script that were used in the creation of this report can be found via the following link: https://1drv.ms/u/s!AimaXOpuZCjEj7lTS8gOXVB7GPOaGA?e=bf2k6F